DNA Hybridization Assay

DOI: 10.1002/ange.201408403

Increasing Hybridization Rate and Sensitivity of Bead-Based Assays Using Isotachophoresis**

*Hirofumi Shintaku, James W. Palko, Glenn M. Sanders, and Juan G. Santiago**

Abstract: *We present an electrokinetic technique to increase the reaction rate and sensitivity of bead-based assays. We use isotachophoresis (ITP) to preconcentrate and co-focus target molecules and beads into a single ITP zone. The process achieves rapid mixing, stirring, and strongly increases the binding reaction rate. We demonstrate our assay with quantitative detection of 24 nt single-stranded DNA over a dynamic range of three orders of magnitude and multiplexed detection of ten target species per sample. We show that ITP can achieve approximately the same sensitivity as a well-stirred standard reaction in 60-fold reduced reaction time (20 min versus 20 h). Alternately, compared to standard reaction times of 30 min, we show that 20 min ITP hybridization can achieve 5.3-fold higher sensitivity.*

Probe methods such as planar microarrays[1] and bead-based suspension arrays[2] are attractive for molecular diagnostic applications because of their ability to achieve multiplexing and their customizability. The bead suspension format supports lower levels of multiplexing than planar arrays, with approximately several hundred distinguishable bead codes.[2] This level of multiplexing, however, is sufficient for the vast majority of clinical applications,[3] and the format offers a number of practical advantages including lower cost than microarrays[4] and high reconfigurability. (New "array" combinations can be achieved by selecting and mixing beads from a library.)

Beads also possess an intrinsic physical advantage to planar substrates in that they distribute the probe molecule throughout the sample volume, thereby reducing the length scale for target transport. Therefore, in some applications, bead assays offer shorter hybridization duration ($\approx$30 min) compared to microarrays (15–24 h).[5] Despite this improved mixing, bead assays nevertheless require similar hybridization duration to achieve comparable limits of detection as microarrays.[6] This implies that accelerating the slow reaction of low abundant targets remains a challenge.

Isotachophoresis (ITP) is an electrokinetic technique for producing high concentration factors of ionic analytes using a heterogeneous buffer system, composed of a leading electrolyte (LE), and a trailing electrolyte (TE).[7] In peak-mode ITP,[8] multiple analytes (e.g., beads and target) sharply focus at a TE-to-LE interface resulting in a significant increase of the concentration of analytes (up to million-fold increases are possible within 2 min under ideal conditions[9]). This rapid mixing, co-focusing, and preconcentration can be used to accelerate second-order chemical reactions such as DNA hybridization.[10] Bercovici et al. presented a detailed study of the homogeneous DNA hybridization dynamics under ITP focusing and demonstrated 14000-fold reduction in hybridization time.[11] Bahga et al. demonstrated a duplex assay by integrating ITP-based rapid DNA hybridization and capillary zone electrophoresis.[12] ITP can also enhance the surface hybridization reaction between a suspended target and an immobilized probe.[13] Recently, ITP was used to accelerate selective capture (and recovery) in affinity chromatography[14] and to achieve 30 min reactions in a multiplexed surface microarray (20 species and 60 reaction spots).[15] The latter work being, to our knowledge, the first truly multiplexed (e.g., more than two) reactions accelerated using ITP. There have also been studies showing that nano- and microparticles can be focused and carried along with an ITP zone.[16] However, no studies combining ITP-enhanced reactions and bead assays by co-focusing target and beads in an ITP zone are known to us.

In this paper, we leverage ITP to concentrate dilute target DNA and co-focus it with beads to strongly accelerate DNA hybridization in a bead suspension assay. Figure 1 shows a schematic of our ITP-aided bead hybridization experiment. We use a simple one-inlet, one-outlet channel architecture and three buffers: LE, a buffering leading electrolyte (BLE), and TE (see S-1 in the Supporting Information (SI) for detailed materials and methods). The LE contained the ssDNA targets and initially filled the entire microchannel. We then injected the magnetic bead suspension into the near-entrance region of the microchannel, and collected these into the channel with an external magnet. The bead suspension contained ten sets of beads each with a unique immobilized DNA probe sequence. We then loaded TE and BLE into the input and the output wells, respectively, and placed platinum wire electrodes into the each well.

[*] Dr. H. Shintaku, Dr. J. W. Palko, Prof. J. G. Santiago
Department of Mechanical Engineering, Stanford University
Stanford, California 94305 (USA)
E-mail: juan.santiago@stanfod.edu
Dr. H. Shintaku
Department of Micro Engineering, Kyoto University
Nishikyo, Kyoto 615-8540 (Japan)
Dr. G. M. Sanders
SomaLogic, Inc.
Boulder, Colorado 80301 (USA)

[**] We gratefully acknowledge Y. Sato and N. Hatano, Kyoto University Machine Shop, for fabricating microfluidic chips. We gratefully acknowledge funding from the National Science Foundation under CBET-1159092. H.S. acknowledges funding from JSPS under 22686021, 26289035, and 26630052. H.S. was supported by fellowships from the John Mung Program of Kyoto University and the Marubun Research Promotion Foundation (Japan).

Supporting information for this article is available on the WWW under http://dx.doi.org/10.1002/anie.201408403.

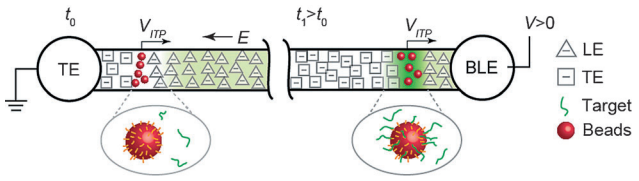

Figure 1. Schematic of hybridization acceleration by co-focusing beads and target in a single ITP zone. The target is initially mixed into LE and distributed throughout the channel. ITP focusing quickly accumulates beads injected at the left, and transports focused beads through the channel. The ITP zone also recruits target, preconcentrates it, and mixes target and beads, thereby accelerating reactions. Beads are collected at the downstream reservoir with a standard pipette.

We applied 300 μA of constant current along the channel. ITP focuses all beads within the ITP zone within about 1 min. Target was recruited and focused into the ITP zone and continually accumulated during most of the experiment. Secondary flow in ITP effectively mixes beads and target to achieve accelerated and kinetics-limited reaction (see S-2 of SI for ITP dynamics). We turned off the applied electric field as the ITP zone arrived at the output well and then recovered the solution including processed beads from the output well for off-chip detection of fraction of hybridization.

The short injected bead zone focuses quickly and bead surfaces offer a finite number of and effective volume concentration of possible binding sites. Meanwhile, ITP recruitment of target results in the continuous accumulation of target in the ITP zone. This recruitment starts as a linear increase in target concentration, C, but C saturates as the increasing surface reaction rate rises and becomes sufficient to accommodate new influx, resulting in a quasi-steady local target equilibrium. This quasi equilibrium is a balance between influx of target into the ITP zone and reaction rate "sink" within it, and we analyze and quantitatively describe this in the SI (S-4). The essence of this equilibrium is captured by the following relation:

$$C^* = \alpha \tag{1}$$

Here C^* is C normalized by the initial target concentration, C_0 and α is an acceleration factor determined by ITP chemistry, ITP dynamics, the reaction on-rate constant (k_{on}), and the ITP-volume-averaged concentration of binding sites. Given this quasi-equilibrium, we can then describe the fraction of reacted surface sites (normalized by total surface sites), Γ^*, as:

$$\Gamma^* = \alpha/(\alpha + K/C_0)[1-\exp(-(\alpha + K/C_0)T^*)] \tag{2}$$

where K is the dissociation constant, T^* is $k_{on}C_0t$, and t is time. We provide detailed derivation and benchmarking of this ITP-reaction relation in S-5 and S-6. (Refer to S-3 for definition of symbols). We also compare it to an equivalent expression for the well-stirred standard (non-ITP) reaction case, for which the hybridization fraction has the form $\Gamma^*_{std} = 1/(1+K/C_0)[1-\exp(-(1+K/C_0)T^*)]$.

We here highlight two key differences between ITP and the standard, well-stirred reaction case. First, the ITP hybridization fraction contains a prefactor $\alpha/(\alpha+K/C_0)$. For the common case of low abundance target where K/C_0 is much larger than unity, the prefactor becomes $\alpha/(K/C_0)$, and we see that ITP focusing can be interpreted as an increased value of steady state target hybridization fraction (the standard fraction multiplied by α). Second, for the same high K/C_0 regime, we see that the internal quasi-equilibrium dynamics are associated with a rate of reaction accelerated by a factor α. We estimate $\alpha = 18.3$ for our ITP experiments (see S-8 of SI).

We experimentally demonstrate our technique by comparing titration curves for ITP and well-stirred standard reactions. We used ten target-probe pairs composed of commercially available magnetic beads bearing ssDNA probe sequences ($d = 6.5$ μm, MagPlex-TAG microspheres, Luminex, Austin, TX), and perfectly complementary target sequences (see S-1 of SI). We present data for ITP with standard 30 min and standard 20 h hybridizations in Figure 2.

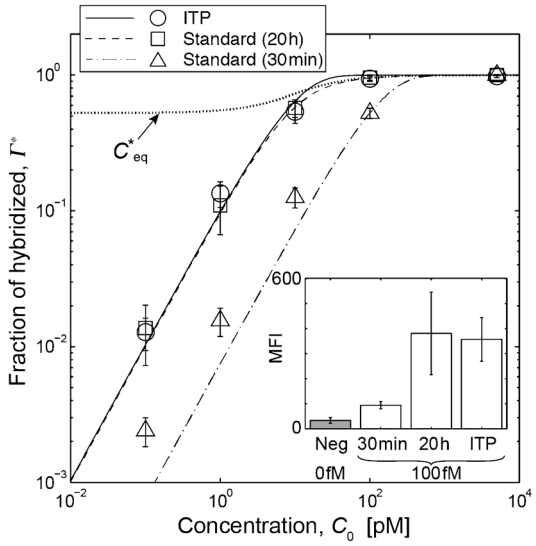

Figure 2. Experimental data demonstrating quantitative detection of a target molecule using 20 min bead-based ITP hybridization and its comparison to well-stirred standard hybridizations performed for 30 min and 20 h. We obtained the titration curves for the concentration of target 8 ranging from 100 fM to 5 nM. Along with experimental data (symbols), we show the prediction of the analytical model for ITP hybridization (solid) with no fitting parameter. We also show results of analytical models for the standard 20 h (broken) and 30 min (dashed-dotted) hybridizations. The range bars in the Figure indicate the standard deviation across repetition ($N = 6$ for standard or $N = 9$ for ITP). The dotted line shows the ideal equilibrium target concentration at standard hybridization conditions. The inset shows raw signals at an initial target concentration of 100 fM and compares these to the negative control (no target).

Here we show representative results for one target (target 8), but include additional results for another target (target 9) in S-9 of the SI. The fluorescent bead signal data for these experiments were obtained using a Luminex 200 instrument (see S-1 of SI). In all cases, the fraction of hybridized probe monotonically increased with increasing concentration over a dynamic range of three orders of magnitude. The fractions of hybridized probe for 20 min ITP hybridization were

comparable to those of standard hybridization for 20 h at all concentrations. ITP hybridization yielded significantly higher fractions hybridized compared to standard hybridization for 30 min, showing the acceleration effect of ITP. For example, in the inset, we compare the raw signal for ITP and standard hybridization cases with the lowest target concentration (100 fM) and negative control of no target in solution. The signal relative to the negative control was 10.7 for ITP, 2.82 for standard 30 min, and 11.4 for standard 20 h, showing 5.3 fold sensitivity increase by 20 min ITP compared to standard 30 min.

We also show the fraction of hybridized probes predicted with our analytically derived Eq. (2) for ITP hybridization and for experimental parameters of $K = 7.3 \times 10^{-12}$ M, $k_{on} = 4.4 \times 10^{6}$ 1/Ms and $\Gamma_{max} = 6$ nmol m^{-2} (see S-6 and S-7). The approximate analytical model yields good quantitative agreement for the observed trends with no fitting parameter. (Model parameters are determined using separate experiments as described in the SI.) As a reference, we also show the predicted equilibrium level of fraction of target hybridized, C^*_{eq}.

Figure 3 shows measurements of specific and nonspecific signals obtained with ITP, standard hybridization at 30 min, and standard hybridization at 20 h for target concentrations between 100 fM and 5 nM. The signals represent the averaged median fluorescence intensity (MFI) resulting from specific binding of ssDNA to the matched probe (ID = 8) or nonspecific binding of ssDNA to the mismatched probes (others). Figure 3b further shows plots of the so-called specificity index,[15] defined as the ratio of specific signal versus the highest nonspecific signal (ID = 4 for the case of target 8). (No data is shown for 100 fM as there was no detectable nonspecific signal above background.) The specificity index from ITP and standard 20 h incubation were the same order of magnitude and showed similar trends. ITP yields higher specificity index than standard incubation for target 8 concentrations below 10 pM. We present additional specificity data for target 9 in S-9 in the SI, which shows that ITP can also have slightly lower specificity index at low concentrations. Overall, we concluded that ITP exhibits specificity on par with standard hybridizations. We note Han et al. reached a similar conclusion regarding specificity for their ITP-aided DNA microarray hybridizations.[15]

In summary, we demonstrated the use of ITP to co-focus, mix, and react nucleic acid targets and multiplexed assay beads in suspension. ITP hybridizations lasting only 20 min, produce sensitivities similar to those obtained after 20 h of well-stirred standard hybridizations. 20 min ITP hybridization yields a five-fold enhancement in sensitivity compared to standard assay protocols with 30 min hybridization. ITP-based hybridization has potential to significantly speed up bead hybridizations while also improving their sensitivity.

Received: August 20, 2014
Published online: October 10, 2014

Keywords: DNA analysis · hybridization assay · isotachophoresis · multiplexing

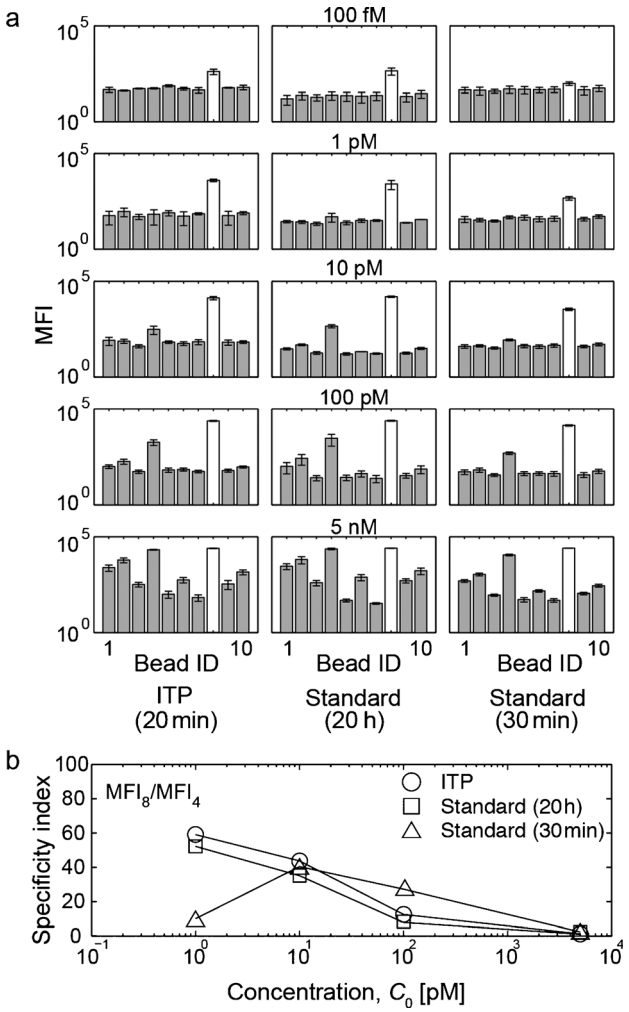

Figure 3. Comparison of specific and nonspecific signal between ITP hybridization and standard incubation (at both 20 h and 30 min). a) Averaged MFI (log scale) for target 8 hybridized with matching probe (bead ID = 8) and nine bead types with non-matching probes. The range bars in the Figure indicate the standard deviation across $N = 3$ for standard cases and $N = 5$ for ITP. b) Specificity index for target 8 (ratio of averaged MFI between specific binding and the highest nonspecific binding (bead ID = 4). Similar data is provided in the SI for target 9.

[1] C. G. Liu, G. A. Calin, S. Volinia, C. M. Croce, *Nat. Protoc.* **2008**, *3*, 563 – 578.
[2] H. Y. Hsu, T. O. Joos, H. Koga, *Electrophoresis* **2009**, *30*, 4008 – 4019.
[3] H. S. Eng, G. Bennett, P. Bardy, P. Coghlan, G. R. Russ, P. T. Coates, *Hum. Immunol.* **2009**, *70*, 595 – 599.
[4] J. Q. Yin, R. C. Zhao, K. V. Morris, *Trends Biotechnol.* **2008**, *26*, 70 – 76.
[5] M. Schmitt, I. G. Bravo, P. J. Snijders, L. Gissmann, M. Pawlita, T. Waterboer, *J. Clin. Microbiol.* **2006**, *44*, 504 – 512.
[6] a) J. Lu, G. Getz, E. A. Miska, E. Alvarez-Saavedra, J. Lamb, D. Peck, A. Sweet-Cordero, B. L. Ebert, R. H. Mak, A. A. Ferrando, J. R. Downing, T. Jacks, H. R. Horvitz, T. R. Golub, *Nature* **2005**, *435*, 834 – 838; b) S. Kraemer, J. D. Vaught, C. Bock, L. Gold, E. Katilius, T. R. Keeney, N. Kim, N. A. Saccomano, S. K. Wilcox, D. Zichi, G. M. Sanders, *PLoS One* **2011**, *6*, e26332.

[7] a) A. Rogacs, L. A. Marshall, J. G. Santiago, *J. Chromatogr. A* **2014**, *1335*, 105 – 120; b) H. Shintaku, H. Nishikii, L. A. Marshall, H. Kotera, J. G. Santiago, *Anal. Chem.* **2014**, *86*, 1953 – 1957.
[8] T. K. Khurana, J. G. Santiago, *Anal. Chem.* **2008**, *80*, 6300 – 6307.
[9] B. Jung, R. Bharadwaj, J. G. Santiago, *Anal. Chem.* **2006**, *78*, 2319 – 2327.
[10] a) G. Goet, T. Baier, S. Hardt, *Lab Chip* **2009**, *9*, 3586 – 3593; b) A. Persat, J. G. Santiago, *Anal. Chem.* **2011**, *83*, 2310 – 2316; c) M. Bercovici, G. V. Kaigala, K. E. Mach, C. M. Han, J. C. Liao, J. G. Santiago, *Anal. Chem.* **2011**, *83*, 4110 – 4117; d) C. Eid, G. Garcia-Schwarz, J. G. Santiago, *Analyst* **2013**, *138*, 3117 – 3120.
[11] M. Bercovici, C. M. Han, J. C. Liao, J. G. Santiago, *Proc. Natl. Acad. Sci. USA* **2012**, *109*, 11127 – 11132.
[12] S. S. Bahga, C. M. Han, J. G. Santiago, *Analyst* **2013**, *138*, 87 – 90.
[13] a) G. Garcia-Schwarz, J. G. Santiago, *Anal. Chem.* **2012**, *84*, 6366 – 6369; b) G. Garcia-Schwarz, J. G. Santiago, *Angew. Chem. Int. Ed.* **2013**, *52*, 11534 – 11537; *Angew. Chem.* **2013**, *125*, 11748 – 11751; c) M. Karsenty, S. Rubin, M. Bercovici, *Anal. Chem.* **2014**, *86*, 3028 – 3036; d) R. Khnouf, G. Goet, T. Baier, S. Hardt, *Analyst* **2014**, *139*, 4564 – 4571.
[14] V. Shkolnikov, J. G. Santiago, *Anal. Chem.* **2014**, *86*, 6229 – 6236.
[15] C. M. Han, E. Katilius, J. G. Santiago, *Lab Chip* **2014**, *14*, 2958 – 2967.
[16] a) U. Pyell, W. Bucking, C. Huhn, B. Herrmann, A. Merkoulov, J. Mannhardt, H. Jungclas, T. Nann, *Anal. Bioanal. Chem.* **2009**, *395*, 1681 – 1691; b) G. Goet, T. Baier, S. Hardt, *Biomicrofluidics* **2011**, *5*, 014109.